Available online at www.sciencedirect.com
SCIENCE DIRECT®
Journal of Chromatography A, 1087 (2005) 95–103
JOURNAL OF CHROMATOGRAPHY A
www.elsevier.com/locate/chroma

Numerical simulation of the chromatographic process for direct ligand–macromolecule binding studies

Claire Vidal-Madjar[a,*], Florentina Cañada-Cañada[a,b], Alain Jaulmes[a], Anastasia Pantazaki[c], Myriam Taverna[b]

[a] *Laboratoire de Recherche sur les Polymères, CNRS, 2 rue Henry Dunant, 94320 Thiais, France*
[b] *Groupe de Chimie Analytique de Paris Sud, Faculté de Pharmacie, 92290 Châtenay-Malabry, France*
[c] *Laboratory of Biochemistry, Aristotle University of Thessaloniki, 54006 Thessaloniki, Greece*

Available online 25 January 2005

Abstract

A numerical simulation of the direct zonal liquid chromatographic method is described for studying the binding of a ligand to a macromolecule by quantification of the interacting species present in a sample at equilibrium. The algorithm accounts for both the kinetic exchanges in solution and the dispersion effects depicted by the Fick law. Dimensionless variables are used for the concentrations which are expressed as a function of the equilibrium constant, K_D. The free ligand concentration was varied in the injected samples from 0.1 to 20 K_D, while that of the macromolecule was kept constant. An apparent binding isotherm was obtained from the total ligand chromatogram generated by the simulation run, when the amount emerging at almost column dead volume is plotted against that eluting at the free ligand retention time.

As a continuous dissociation of the complex may occur during its migration, the apparent binding curve and the theoretical binding isotherm coincide at extremely low dissociating rates. At larger dissociation rates ($0.001\,s^{-1} < k_d < 0.1\,s^{-1}$, for a first peak eluting in 1 min) the simulations were used to test various chromatographic conditions. The flow rate (or column volume) is the major effect which influences the on-column dissociation process as an exponential decay was found when the apparently bound fraction is plotted against the analysis time. The apparent equilibrium coefficient is close to the theoretical one for a binding curve generated with an initial solution containing a relatively low total concentration of binding sites ($\leq K_D$). The apparent stoichiometric term is largely underestimated as its value decreases exponentially at increasing dissociation rates. An extrapolation at extremely short analysis times could be used to determine the stoichiometric coefficient characterizing the binding interaction.

Keywords: Chromatography modelling; Direct zonal separation; Ligand-macromolecule binding; Dissociation kinetics

1. Introduction

Procedures using the direct zonal separation method to study the binding interactions are of great interest because HPLC can rapidly and accurately quantify the species present at equilibrium in the injected solution [1–3]. The direct zonal chromatographic method consists in injecting a pre-incubated mixture of a ligand and a macromolecule into a chromatographic column. The interacting species are separated and the concentrations of bound and free ligand in the sample injected are quantified from the areas of the peaks eluting at the retention volume of each species. As a continuous dissociation of the complex may occur during the elution, the approach is valid only with systems exhibiting sufficiently low dissociation rates. Only few experimental studies [1,4–8] have used this method to measure binding interactions as the approach is limited to stable complexes unaffected by the dilution in the mobile phase.

In a previous work [1], we studied experimentally the DNA-actinomycin interactions by analyzing an apparent binding curve obtained by plotting the amounts of bound and free ligand emerging as peaks from a size-exclusion column. The experimental data were analyzed by comparison with the results obtained by numerical simulation of a separation performed with a size-exclusion column. Although a

* Corresponding author. Tel.: +33 1 49 78 12 31
E-mail address: vidal@glvt-cnrs.fr (C. Vidal-Madjar).

0021-9673/$ – see front matter © 2005 Elsevier B.V. All rights reserved.
doi:10.1016/j.chroma.2005.01.008

slow dissociation of the complexed forms was occurring during the migration in the column, an analysis of the apparent binding curve permitted to determine the equilibrium parameters and the association and dissociation rate constants of the drug–DNA binding reaction.

In the present study, we shall give a detailed description of the model used to simulate the separation by retention on a chromatographic support and propose an approach to determine reliable binding constants. The simulation results will be useful to show how to apply the direct separation method to quantitative binding analyses. Iterative simulations were already described to predict the chromatographic behaviour of a complex which elutes under slow dissociating conditions. The model of Nimmo and Bauermeister [9] which does not account for axial diffusion gives a semi-quantitative description of the elution behaviour of a protein–ligand complex in zonal gel filtration. In the algorithm described by Stevens for size-exclusion chromatography [10], association–dissociation probabilities were used to approximate the intermixing of the free and complexed species during the time intervals.

In the model described here, both association–dissociation kinetics and dispersion effects are accounted for during the species migration in the chromatographic column. The simulation results are used to define the domain of applicability of the direct separation method when apparent binding curves are employed to evaluate the binding parameters of the ligand–macromolecule interaction.

2. Theory

The chromatographic process was simulated by dividing the column into a large number of cross-slices. In each cell, the variations of concentrations as a function of time were calculated by considering two different steps: the kinetic exchanges of the interacting species in solution and the dispersion effects depicted by the Fick law. The migration of the mobile phase was simulated by shifting the mobile phase from a given slice to the following one. The time spent in each slice Δt was deduced from the slice thickness Δz by $\Delta t = \Delta z/u$, where u is the mobile phase velocity. We assume that the retention of all the interacting species are governed by a linear partition isotherm and the retention factor of the ligand is k_L. The macromolecule and the complexed forms elute at the same retention volume, with a retention factor k_A.

2.1. Simulation of the chemical changes in a given slice

The interaction in solution of the macromolecule A with the ligand L was described by a series of chemical equations, according to the scheme:

$$AL_{i-1} + L \rightleftarrows AL_i \tag{1}$$

where i is the number of ligand molecules bound per macromolecule. If Z is the maximum number of bound ligand (stoichiometric coefficient), then $1 < i < Z$. At equilibrium, the concentration of bound ligand x in the mobile phase is related to that of free ligand concentration $[L]$ by the binding isotherm, when assuming equal and independent sites (Scatchard treatment):

$$x = Z[A]_0 \frac{[L]}{K_D + [L]} \tag{2}$$

where $[A]_0$ is the total concentration of the macromolecule in the mobile phase and the total concentration of binding sites is $Z\,[A]_0$. The dissociation equilibrium constant is $K_D = k_d/k_a$ where the dissociation and association rate constants are respectively k_d and k_a.

In each slice, the total concentrations of A and L are:

$$G_A = [A]_0(1 + k_A) \tag{3}$$

$$G_L = [L](1 + k_L) + x(1 + k_A) \tag{4}$$

The kinetic law governing the association–dissociation process is then in each slice:

$$(1 + k_A)\frac{dx}{dt} = k_a[L](Z[A]_0 - x) - k_d x \tag{5}$$

Eq. (5) may be written as follows:

$$\frac{dx}{dt} = r_a(g_1 - x)(Z[A]_0 - x) - r_d x \tag{6}$$

where $g_1 = G_L/(1 + k_A)$, $r_a = k_a/(1 + k_L)$ and $r_d = k_d/(1 + k_A)$.

The solution of Eq. (6) is given by:

$$\frac{1}{x - x^*} = \frac{e^{r_a E t}}{x_0 - x^*} - \frac{e^{r_a E t} - 1}{E} \tag{7}$$

where x is equal to the equilibrium value x^* and for $t = 0$, $x = x_0$. The other auxiliary variables are expressed as follows: $E = \sqrt{(g_2)^2 - 4g_1\,Z[A]_0}$ and $g_2 = g_1 + Z[A]_0 + K_D(1 + k_L)/(1 + k_A)$

The concentration of bound ligand at equilibrium is given by:

$$x^* = \frac{(g_2 - E)}{2} \tag{8}$$

The above solution was applied to calculate the evolution of mobile and stationary phase compositions after a time $t = \Delta t$ in each slice, the time needed by the mobile phase to flow through the volume of one slice.

2.2. Simulation of the mobile phase progression during the time increment

The simulation algorithm proceeds from the outlet to the inlet of the column. During the time increment Δt, the total concentration in the jth cell is deduced from the previous one by:

$$G_L'(j) = [L](j - 1) + k_L[L](j) + x(j - 1) + k_A x(j) \tag{9}$$

$$G_A'(j) = [A]_0(j - 1) + k_A[A]_0(j) \tag{10}$$

For each slice, the new total concentration of the macromolecule in solution after mobile phase progression is then:

$$[A]_0 = \frac{G_A{}'(j)}{(1+k_A)} \tag{11}$$

The new initial value of the bound ligand concentration in solution x_0 is calculated from:

$$x_0 = \frac{k_A x(j) + x(j-1)}{(1+k_A)} \tag{12}$$

2.3. Simulation of the dispersive effects in a given slice

The global dispersive effect was accounted for by applying the Fick law to the concentrations of each species in solution. All contributions to band broadening as molecular diffusion, eddy diffusion, kinetic mass transfers were assumed to be described by a global apparent diffusion coefficient D'.

For a given solute, the molar rate μ through a cross section S of the column is given by the Fick law [11]:

$$\mu = -SD'\frac{\partial C}{\partial z} \tag{13}$$

where C the concentration of the solute considered. The molar rate is related to the concentration increment $\Delta_d C$ by the equation:

$$\mu \approx -\Delta_d C\frac{\Delta V_0}{\Delta t} \tag{14}$$

where ΔV_0 is the mobile phase volume of a slice.

For the inner cross sections, we have for $\Delta_d C$:

$$\Delta_d C \approx SD'\frac{\Delta t}{\Delta V_0}\frac{\partial C}{\partial z} \approx \frac{D'}{u}\frac{\Delta_s C}{\Delta z} \tag{15}$$

where $\Delta_s C$ is the difference of concentration in two vicinous slices. When j varies from 0 to $(n-1)$, for each section $\Delta_d C$ is given by:

$$\Delta_d C(j\Delta z) = \frac{D'}{u\Delta z}(C(j+1) - C(j)) \tag{16}$$

where $C(0)$ is the concentration injected. From this expression one can deduce the evolution of the concentration in any slice, during the time increment Δt. For the inner slices, we have

$$\begin{aligned}\Delta C(j,t) &= \Delta_d C(z) - \Delta_d C(z-\Delta z)\\ &= \frac{D'}{u\Delta z}[C(j+1) + C(j-1) - 2C(j)]\end{aligned} \tag{17}$$

For the first and last lice, the equations are:

$$\Delta C(1,t) = \Delta_d C(\Delta z) = \frac{D'}{u\Delta z}[C(1) - C(0)] \tag{18}$$

$$\Delta C(n,t) = \Delta_d C(n\Delta z - \Delta z) = \frac{D'}{u\Delta z}[C(n) - C(n-1)] \tag{19}$$

2.4. Numerical procedure

The numerical procedure consists of calculation loops, every one establishing the concentrations C' of each species for the instant $(t+\Delta t)$ from those for the instant (t). Inside every loop the algorithm was divided into two major steps, one for calculating the concentration changes due to global axial dispersion according to the approximate Fick law and the other for the kinetic exchanges in the solution. For each step, the mass conservation was strictly maintained. The number of slices N was chosen large enough to minimize numerical dispersion. The slice liquid volume is $\Delta V_0 = V_0/N$, where V_0 is the mobile phase volume of the column.

The initial conditions correspond to the injection of a rectangular step of a preincubated mixture. At $t = 0$, the column was with zero concentrations in both phases. We have for the initial conditions, when $0 < t < t_i$: Z $[A]_0 = c_s$, $[L] = c_i$ and $x = q_i$ where c_s is the total concentration of binding sites in the sample injected. The concentration of bound ligand q_i of the pre-incubated mixture is related to that of the free ligand c_i by the equilibrium binding isotherm given by Eq. (2).

Unless indicated, the simulation runs were performed with the following chromatographic conditions: volume of mobile phase in a column, $V_0 = 1\,\text{cm}^3$; flow rate, $\delta = 1\,\text{cm}^3\,\text{min}^{-1}$; apparent global diffusion coefficient, $D' = 0.001\,\text{cm}^2\,\text{s}^{-1}$; retention factors, $k_A = 0.01$ and $k_L = 3$; injected sample volume $0.02\,\text{cm}^3$. The simulation program was written in Fortran language and was run on a PC computer. A non-linear least square fit program (Origin software, Microcal Software, Northampton, MA, USA) was used to determine the coefficients of the apparent binding curves.

3. Results and discussion

The simulation describes the separation of a mixture containing the ligand and the macromolecule at equilibrium in a sample injected into a chromatographic column. The macromolecule and its associated forms are assumed to elute as non-retained species at almost column dead volume, while the ligand is retained with a retention factor k_L. Unless specified, the simulations were performed under the HPLC conditions previously given and the elution time of a non-retained compound is generally $t_0 = 1$ min.

The experimental conditions of the pre-incubated solution are assumed to be kept during the separation in the chromatographic column. The temperature of the column is thus equal to that used for equilibrating the species in the injected solution. Similarly, the same solvent is used for both the sample and the mobile phase eluent. The association–dissociation process between the interacting species is thus governed by the same kinetic law in the injected mixture at equilibrium and during column migration. The total ligand chromatogram profile is the result of the association–dissociation kinetics and the equilibrium isotherm (Eq. (2)) characterizing the binding affinity of the ligand to the macromolecule in the

solution injected. With a sufficiently slow dissociation process, an apparent binding curve can be obtained by plotting the amount emerging as a first peak against that eluting at free ligand retention volume. It is close to the equilibrium binding isotherm for extremely low dissociation rates.

For these binding studies the total concentration of the macromolecule in the sample was kept constant, while that of the free ligand concentration was varied from 0.1 to 20 K_D in order to study a wide range of situations in which 9–95% of the macromolecule binding sites are saturated. The concentrations are expressed as a function of K_D in order to handle dimensionless variables. This approach permits to predict a chromatographic behaviour independently from the value of the ligand–macromolecule affinity constant.

Examples with a low and a large total concentration of binding sites in the starting solution will be given. In the range $c_s \leq K_D$, the concentration of the bound ligand is relatively low compared to that of the free compound, and the dissociation of the first peak does not contribute significantly to the amount eluted in the second one. As shown in next section a different chromatogram is obtained at larger c_s values. An example of a large total concentration of binding sites in the initial sample will be studied by selecting $c_s = 10\,K_D$. With this highly concentrated macromolecule solution, the ligand amount which dissociates from the first peak is sufficiently large to alter the total ligand chromatogram.

3.1. Influence of the dissociating effect on the total ligand chromatogram

In presence of a slow dissociation process, the chromatogram of the total ligand concentration shows two peaks, one eluting at column dead volume and the other at the retention time of the free ligand (Fig. 1). The bound species coelute in the first peak with the macromolecule. The areas of the first and second peak are not equal to the amounts of free and bound ligand present at equilibrium in the injected solution, except for extremely low dissociation rates ($k_d < 0.0005\ s^{-1}$, for $t_0 = 1$ min). At increasing k_d values, the area of the first peak decreases, while an increase of the baseline level between the first and the second peak is observed. With large dissociation rates, the first peak totally disappears and the area of the second peak increases.

At diluted concentrations in the sample injected ($c_s = K_D$ and $c_i = 0.1\,K_D$), the peak profiles of the total chromatogram (Fig. 1a) are altered only when relatively large dissociation rates are considered ($k_d \geq 0.05\ s^{-1}$), i.e. for dissociation time and first peak elution time of the same magnitude order. With sufficiently large free ligand concentrations to saturate at equilibrium the binding sites of the macromolecule in the initial sample, the peak shapes are not significantly modified (Fig. 1b), even at a relatively large dissociation rate as $k_d = 0.1\ s^{-1}$. In the example of Fig. 1, the total ligand profile is generally not markedly altered because a relatively low amount arises from the bound fraction which dissociates during its migration through the column.

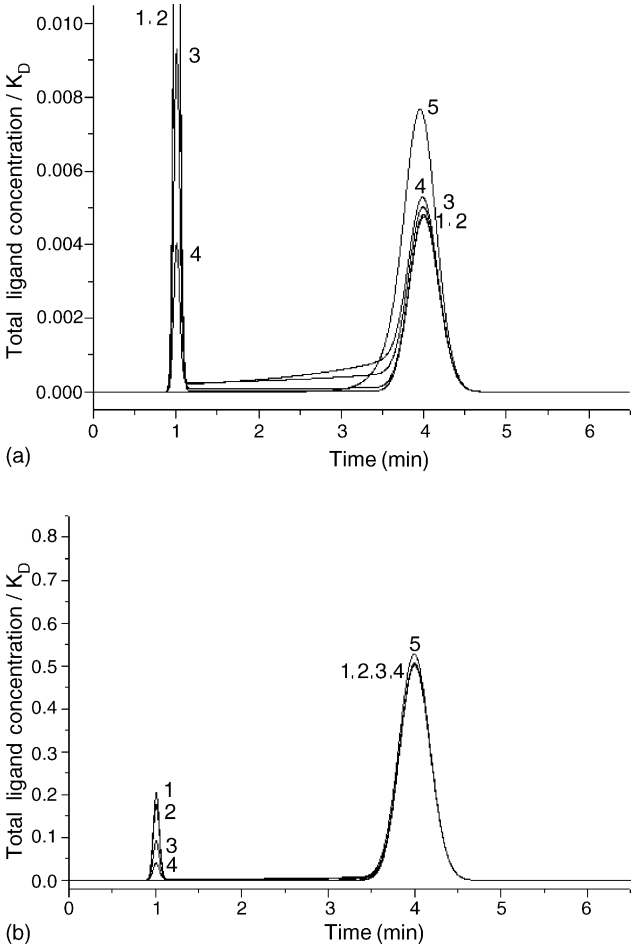

Fig. 1. Total ligand profiles as a function of the dissociation rate constant. Simulations with an initial mixture containing at equilibrium a low binding site concentration ($c_s = K_D$) and (a) a low ($c_i = 0.1\,K_D$) or (b) a large ($c_i = 11\,K_D$) free ligand concentration. Chromatographic conditions: $V_0 = 1$ mL, $k_A = 0$, $k_L = 3$, $D' = 0.001\ cm^2\ s^{-1}$, flow rate 1 mL/min. dissociation rate constants: $k_d\ (s^{-1}) = 0.001$ (1); 0.01 (2); 0.05 (3); 0.1 (4); 1 (5).

A different total ligand chromatogram is generated when the concentrations of binding site in the initial solution is large, as illustrated in Fig. 2 with $c_s = 10\,K_D$. The injected concentration of binding sites is much larger than that of the free ligand ($c_i = 0.1\,K_D$). For this example, the contribution of the dissociated amount to the area of the second peak can be significant, specially at low injected concentrations of free ligand (Fig. 2a). At large free ligand concentrations in the sample mixture ($c_i = 11\,K_D$ in Fig. 2b), the decrease of the first peak due to the dissociation process contributes to a much less extent to the increase of the second peak area.

The above simulation results are illustrated in Fig. 3, which gives the evolution with the dissociation rate of the fraction eluted in the first (Fig. 3a) and second peaks (Fig. 3b), calculated as the ratio of the areas divided by respectively the amounts of bound and free ligand present at equilibrium in the injected mixture. The apparently bound fraction decreases exponentially at increasing values of k_d (Fig. 3a).

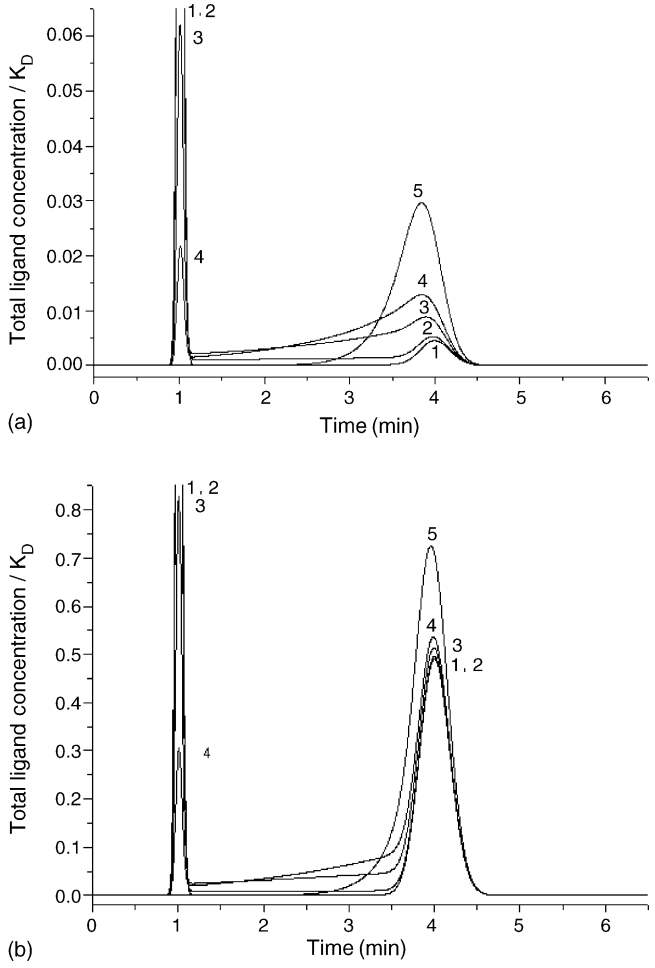

Fig. 2. Total ligand profiles as a function of the dissociation rate constant. Simulations with an initial solution containing at equilibrium a large binding site concentration ($c_s = 10\,K_D$) and (a) low ($c_i = 0.1\,K_D$) or (b) large ($c_i = 11\,K_D$) free ligand concentrations. Same chromatographic conditions and dissociation rates as in Fig. 1.

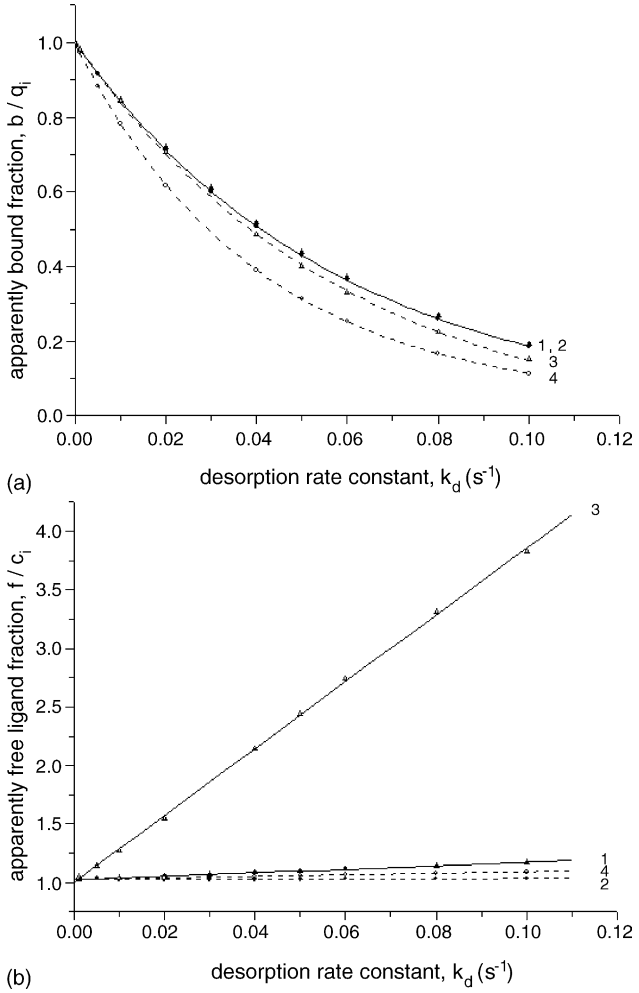

Fig. 3. Variation of the fraction eluted in (a) first or (b) second peak as a function of the dissociation rate constant. Simulation results with low (solid lines) and large (dotted lines) concentrations of binding sites in the initial solution concentrations at equilibrium in the injected sample: $c_s = K_D$ and $c_i = 0.1\,K_D$ (1); $c_s = K_D$ and $c_i = 20\,K_D$ (2); $c_s = 10\,K_D$ and $c_i = 0.1\,K_D$ (3); $c_s = 10\,K_D$ and $c_i = 20\,K_D$ (4). Same chromatographic conditions as in Fig. 1.

The variations are nearly the same whatever the concentrations of the interacting species present at equilibrium in the starting solution (binding sites or free ligand concentrations).

For a large free ligand concentration in the initial solution, the increase of the second peak area at increasing K_D values is small (Fig. 3b). There is a discrete modification of peak areas at both low and large concentration of binding sites in the starting sample (plots 2 and 4). With diluted injected concentrations of the free ligand and the macromolecule ($c_i = 0.1\,K_D$ and $c_s = K_D$), a small linear increase at larger dissociation rates is also displayed (plot 1 in Fig. 3b). With a low free ligand concentration ($c_i = 0.1\,K_D$) and a large binding site concentration in the initial sample ($c_s = 10\,K_D$), a strong variation with the dissociation rate values is observed, and the slope of the straight line (plot 3) is significantly higher than the one observed with $c_s = K_D$ (plot 1). The variations of the second peak fractions with the dissociation rate values illustrated in Fig. 3b for a low and a large binding site concentrations, summarize the modifications already observed at fast dissociation kinetics when comparing the total ligand chromatograms of Figs. 1 and 2.

3.2. Apparent binding equilibrium isotherm

An apparent binding curve was obtained by plotting the area of first peak against that of the second one. The amounts eluted were divided by the volume of sample injected in order to handle apparent bound and free concentrations (b and f). These concentrations are equal to those of the starting solution (q_i and c_i), when there is no column dissociation effect, i.e. at extremely low dissociation rates ($k_d \approx 0$). When using the dimensionless variables b/c_s and f/K_D, the apparent binding curve is given by:

$$\frac{b}{c_s} = \frac{\alpha f/K_D}{\beta + f/K_D} \tag{20}$$

where α and β are coefficients equal to unity if the apparent binding curve is identical to the theoretical equilibrium isotherm characterizing the interaction at equilibrium of the species in solution (Eq. (2)). As explained above, the binding curves were generated by varying the free ligand concentration of the injected sample from 0.1 to 20 K_D, while that of the macromolecule was kept constant. Two different total binding site concentrations were considered with a low and a large c_s value ($c_s = K_D$ and 10 K_D). The effect of the dissociation rate constant on the apparent binding curves was studied and Fig. 4 illustrates the decrease of the asymptotic plateau at increasing dissociation rate constants, with $c_s = K_D$ in the various samples injected.

At extremely low k_d values ($k_d < 0.0005\ s^{-1}$ for $t_0 = 1$ min), the dissociation due to the column dilution effect can be neglected. In these conditions, the areas of bound and free ligand are respectively equal to those present at equilibrium in the initial solution and the apparent binding isotherm nearly coincides with the theoretical one (dotted line in Fig. 4). At larger k_d values, the area of the first peak is decreasing, with higher level of the base line between the first and the second peak (Figs. 1 and 2). With $k_d \leq 0.1\ s^{-1}$ an apparent binding curve can be generated by plotting the area of first peak against that of the second one at various free ligand concentrations in the injected sample. For simulations performed with an almost instantaneous equilibrium between the interacting species ($k_d > 0.5\ s^{-1}$), the first peak has vanished (Figs. 1 and 2). With these conditions, the complexed forms are totally dissociated during the migration through the column and a plot of the apparent binding curve is not possible.

In Table 1 are compared the coefficients α and β determined by fitting Eq. (20) to the apparent binding curves generated at different dissociation rate constants. For a low c_s value, the equilibrium term β is only slightly overestimated.

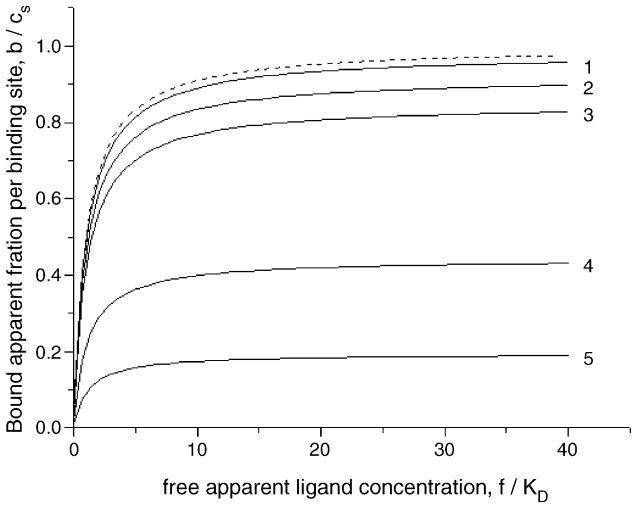

Fig. 4. Influence of the dissociation rate constant on the apparent binding curve. Binding site concentration in the initial sample: $c_s = K_D$ dotted line: theoretical equilibrium isotherm solid line: apparent binding curves generated with the dissociation rates: k_d (s^{-1}) = 0.001 (1); 0.005 (2); 0.01 (3); 0.05 (4); 0.1 (5) and the same chromatographic conditions as in Fig. 1.

Table 1
Influence of the dissociation rate constant on the parameters of the apparent binding isotherm

k_d (s^{-1})	α	β	α	β
0.001	0.982	1.026	0.983	1.047
0.005	0.920	1.033	0.925	1.136
0.01	0.849	1.041	0.850	1.251
0.05	0.442	1.095	0.430	2.238
0.1	0.194	1.140	0.171	3.352
Total binding site concentration in the sample	$c_s = K_D$ (mol L^{-1})		$c_s = 10\ K_D$ (mol L^{-1})	

Simulations performed with a low and a large binding site concentration in the initial sample and the same chromatographic conditions as in Fig. 1.

A discrete variation is noticed at increasing k_d values, but even for relatively large dissociation rate constants ($k_d = 0.1\ s^{-1}$) the difference with the theoretical value never exceeds 15%. A different behaviour is obtained when a large c_s concentration is used in the injected samples (Table 1). A strong increase of β at increasing dissociation rates is observed as this term is more than 25% times above the expected value with $k_d = 0.01\ s^{-1}$. At high reaction rates and large c_s concentrations, a direct determination of K_D from the β value is not suitable, considering the important modifications in peak shape of the second elution peak (Fig. 2a). These results show that a good estimation of the equilibrium constant K_D is generally obtained from the analysis of the apparent binding curve, when samples with a low concentration of binding sites are considered ($c_s \leq K_D$). At larger c_s concentrations, the value of the apparent equilibrium term will be close to unity only with systems having low enough kinetic rates.

For the apparent stoichiometric term α, its value is underestimated but there is no significative difference between the simulations carried out at low and large binding site concentrations in the starting solution (Table 1). Such effect was previously illustrated in Fig. 3, where the decrease of the first peak amount at increasing dissociation rates is nearly the same whatever the total concentration of binding sites in the preincubated solution. Fig. 4 shows the strong decrease of the level of the asymptotic plateau and thus of the α value at larger dissociation rate values. When plotted as a function of the k_d value, the variation is that of an exponential decay similar to the plots of Fig. 3a which shows the evolution of the bound fraction (first peak area versus k_d). A direct determination of the stoichiometric coefficient Z from the apparent term may be difficult because there is pronounced decrease of α at relatively moderate dissociation rates ($0.01 < k_d < 0.1\ s^{-1}$ in Table 1).

In "real" experiments, the effect of noise and base line drifts will affect the precision on the peak area measurements and increase the error intervals when evaluating the binding coefficients from the apparent binding curve. This effect is specially important for the apparent equilibrium coefficient as a number of points in the low concentration range of the apparent binding curve ($f < 5\ K_D$) is needed for an accurate determination of the β coefficient. Moreover, the area of the

second peak in the total ligand profile may be difficult to measure accurately, as the ligand is often retained as a broad and tailing peak. For the apparent stoichiometric coefficient (α), the error made on its determination is lower as it is obtained from the asymptotic value of the first peak area when there is an excess of free ligand concentrations ($f > 10\,K_D$) in the starting sample. This area is generally easier to measure accurately since the bound species elute as a narrow peak at column dead volume. Nevertheless, a selective detection should be used for recording the total ligand chromatogram to eliminate the other perturbations as the macromolecule and impurity signals.

As shown from the simulation results, the equilibrium affinity constant can be relatively well estimated from the apparent binding curve, if the concentration of binding sites is low ($c_s \leq K_D$). This condition may imply to use relatively diluted ligand–macromolecule mixtures. In "real" experiments, such a requirement may be difficult to achieve at ligand detection limits near the base-line noise level. Therefore, a highly sensitive and selective detection system should be used to directly determine the equilibrium affinity constant from the apparent binding curve.

3.3. Influence of the chromatographic conditions on the apparent binding process

The simulations permit to test the various experimental conditions which may influence the on-column dissociation process. We have mainly studied the changes in the time of analysis by varying the flow rate or the column dead volume. The variations of the ligand retention factor were also tested and a small influence on the areas of the peaks of the total ligand chromatogram was noticed. For the global dispersion coefficient used in the simulations, its modification affects the band broadening of the peaks in the total ligand chromatogram, but its effect on peak areas and thus on the results of Table 1 can be neglected.

The time needed by the complex to flow through the column has a strong influence on the coefficients of the apparent binding curve. As in this work, the associated forms were assumed to elute as non-retained compounds, the amount eluting as a first peak was studied as a function of t_0, the elution time of a non-retained compound. This variation was obtained by either changing the flow rate, δ or the column dead volume, V_0.

Typical plots are given in Fig. 5 for various values of the dissociation rate constant. The variations of $\log(b/q_i)$ versus V_0/δ are well described by straight lines, with a slope increasing with the k_d values used in the simulation runs. The data listed in Table 2, indicate that the apparently bound amount b_0 extrapolated for $V_0/\delta = 0$ is almost equal to the concentration present in the initial sample q_i. When the injected free ligand concentration is large as those used in the simulations of Fig. 5, the extrapolation at large flow rates or small column volumes could be used to determine the maximum amount of bound ligand and thus the stoichiometry of the binding

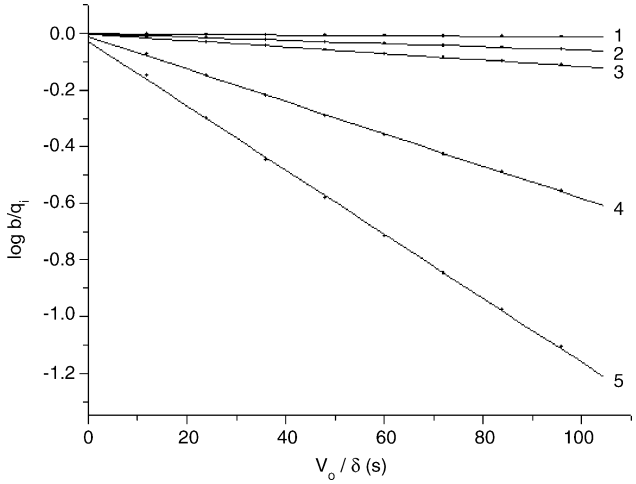

Fig. 5. Linear plot of the logarithm of the apparently bound fraction against the elution time of a non-retained compound. Concentrations at equilibrium in the injected sample: $c_s = K_D$ and $c_i = 20\,K_D$. Simulations generated with the dissociation rates: k_d (s^{-1}) = 0.001 (1); 0.005 (2); 0.01 (3); 0.05 (4); 0.1 (5) and the same chromatographic conditions as in Fig. 1.

chemical reaction. In Table 2, the slope p of the straight lines was determined by plotting $\ln(b/q_i)$ against V_0/δ. As shown in Table 2 for $k_L = 3$ and relatively low dissociation rates, the slope is roughly proportional to the k_d value. Such a dependence was to be expected as it has been shown previously that the plot of the apparently bound fraction against the value given to the dissociation rate is an exponential decay (Fig. 3).

Comparison of the parameters of the apparent binding curve obtained at three different flow rates (0.5, 1 and 2 $cm^3\,min^{-1}$) permit to test the influence of the time of analysis on the column dissociation process (Table 3). In this example, the injected mixture contains a low concentration of binding sites ($c_s = K_D$). As expected for this relatively low c_s value, a negligible influence of the flow rate on the equilibrium term β is found. At all the dissociation rate values studied ($k_d \leq 0.1\,s^{-1}$), the equilibrium coefficient K_D is well determined from the direct analysis of the apparent binding curve. For the stoichiometric term α, a strong influence of the flow rate is found when both the dissociation time and t_0 are of the same magnitude order. With an initial sample containing a macromolecule with nearly all its sites saturated by the

Table 2
Effect of ligand retention on the parameters of the straight lines (Fig. 5) obtained by plotting the logarithm of the fraction eluted as a first peak against the retention time of an unretained compound, with $\ln(b/q_i) = \ln(b_0/q_i) + p(V_0/\delta)$

k_d (s^{-1})	b_0/q_i	p (s^{-1})	b_0/q_i	p (s^{-1})
0.001	0.998	0.00027	0.999	0.00019
0.005	0.997	0.0013	0.998	0.00081
0.01	0.994	0.0026	0.997	0.0016
0.05	0.987	0.016	0.988	0.0080
0.1	0.937	0.065	0.975	0.016
Retention factor	$k_L = 3$		$k_L = 6$	

Simulations performed at almost binding site saturation (same conditions as in Fig. 5).

Table 3
Influence of the chromatographic conditions on the parameters of the apparent binding isotherm

k_d (s^{-1})	α	β	α	β	α	β	α	β
0.001	0.966	1.037	0.982	1.026	0.989	1.020	0.988	1.025
0.005	0.850	1.044	0.920	1.033	0.959	1.016	0.951	1.028
0.01	0.723	1.053	0.849	1.041	0.958	1.023	0.907	1.031
0.05	0.199	1.108	0.442	1.095	0.661	1.054	0.617	1.058
0.1	0.040	1.158	0.194	1.140	0.435	1.082	0.379	1.085
V_0/δ (min)	0.5		1		2		1	
Ligand retention	$k_L = 3$		$k_L = 3$		$k_L = 3$		$k_L = 6$	

Simulations with a low binding site concentration, $c_s = K_D$ (mol L^{-1}).

ligand (Fig. 5), the extrapolation of the asymptotic plateau (or α term) at extremely fast analysis times could be used to determine the stoichiometric parameter Z.

The effect of ligand retention was also studied by comparing the simulation results performed at the same flow rate ($t_0 = 1$ min) with two different ligand retention factors ($k_L = 3$ and 6). At a given dissociation rate constant, the slope of the straight lines obtained by plotting ln (b/q_i) against the elution time of a non-retained compound is significantly lower with $k_L = 6$ (Table 2). For all the k_d values tested with $k_L = 6$, there is a rough proportionality between the slope p and the dissociation rate constant k_d. When comparing the slopes obtained at different k_L values, the lower p value found with $k_L = 6$, is explained by the global rate expression (Eq. (6)) which implies that the larger is the ligand retention factor k_L, the lower is the apparent reassociation process occurring during the migration of the interacting species. When comparing the parameters of the apparent binding curves obtained at two different k_L values (Table 3), the influence of the second peak retention factor on the apparent binding curve is small. Nearly equal apparent equilibrium terms are found at a given dissociation rate constant, and the values are close to unity. A larger apparent stoichiometric term is found with $k_L = 6$, but the difference is significative at only fast dissociation kinetics when $k_d > 0.01\ s^{-1}$.

The effect of flow rate on the apparently bound amount (area of first peak) may be interesting to study as an extrapolation at fast analysis times could be used to determine the concentration of bound ligand in the injected sample. With an excess of free ligand in the initial solution, the extrapolated value is close to the asymptotic plateau of the equilibrium binding isotherm. This study could also be useful for evaluating the kinetic rate constants (k_d and thus k_a if K_D is determined) as the simulations predict an exponential decay for the variation of the amount detected in the first peak versus the analysis time. The coefficient of this exponential curve mainly depends on the kinetics of the binding chemical reaction (k_d value) and on the chromatographic conditions of the separation (ligand retention factor).

4. Conclusion

The simulation of the direct zonal chromatographic method provides a convenient way for studying the dissociation process of the bound species during their migration through the column. It is useful for defining the domain of validity in which one can use an apparent binding curve to determine the equilibrium parameters of a binding chemical reaction. This curve is obtained by analyzing the total ligand chromatogram which exhibits two distinct peaks if the dissociation kinetics are slow enough.

The apparent equilibrium coefficient is generally close to the theoretical equilibrium constant for diluted mixtures containing a low concentration of binding sites in the initial solution ($c_s \leq K_D$). This upper value for the concentration of binding sites in the initial solution implies the detection of the bound species at a level which may be lower than the detection limits. In this case, relatively large concentrations of binding sites in the pre-incubated mixture should be injected in the column and the equilibrium affinity constant can be evaluated by comparison with the total ligand chromatogram obtained by simulating the chromatographic process.

Except for extremely slow dissociation processes, the apparent stoichiometric term largely underestimates the maximum number of ligand molecules bound per macromolecule, as an exponential decrease was found at increasing dissociation rates. An extrapolation of the apparently bound amount at zero elution times could be used to determine the concentration effectively present at equilibrium in the injected solution. This method could be used to determine the stoichiometric coefficient by analyzing the separation profile of a mixture containing an excess of free ligand. A study of the on-column dissociation process at different flow rates offers a promising approach for determining the dissociation rates.

5. Nomenclature

b	bound apparent ligand concentration in the sample injected (mol L^{-1})
b_0	value of b extrapolated at $t_0 = 0$ (mol L^{-1})
c_s	total concentration of the macromolecule binding sites in the sample injected (mol L^{-1})
c_i	free ligand concentration in the sample injected (mol L^{-1})
C	concentration of each species in the mobile phase of a column slice (mol L^{-1})

D' global apparent diffusion coefficient ($cm^2\ s^{-1}$)
E $\sqrt{(g_2)^2 - 4g_1 Z[A]_0}$
f free apparent ligand concentration in the sample injected ($mol\ L^{-1}$)
g_1 $G_L/(1 + k_A)$
g_2 $g_1 + Z[A]_0 + K_D(1 + k_L)/(1 + k_A)$
G_A total concentration of the macromolecule and its complexes in a column slice ($mol\ L^{-1}$)
G_L total concentration of ligand in a column slice ($mol\ L^{-1}$)
k_A capacity factor of the macromolecule and its complexes
k_L capacity factor of the ligand
k_a association rate constant ($L\ mol^{-1}\ s^{-1}$)
k_d dissociation rate constant (s^{-1})
K_D dissociation equilibrium constant ($mol\ L^{-1}$)
N number of slices
p slope of the straight line: $\ln(b/q_i) = \ln(b_0/q_i) + p(V_0/\delta)$ (s^{-1})
q_i bound ligand concentration in the sample injected ($mol\ L^{-1}$)
r_a global association rate constant ($L\ mol^{-1}\ s^{-1}$)
r_d global dissociation rate constant (s^{-1})
S column cross section (m^2)
t time (s)
t_0 elution time of a non-retained compound (s)
u mobile phase velocity along column length ($cm\ s^{-1}$)
V_0 mobile phase volume of the column (cm^3)
x concentration of bound species in a slice at time t ($mol\ L^{-1}$)
x^* concentration of bound species in a slice at equilibrium ($mol\ L^{-1}$)
x_0 concentration of bound species in a slice at time $t = 0$ ($mol\ L^{-1}$)
z distance along column length (cm)
Z stoichiometric coefficient or maximal number of ligand molecules bound to the macromolecule
[species] concentration of the indicated species in a column slice
$[species]_0$ total concentration of the indicated species in a column slice
α apparent stoichiometric term
β apparent equilibrium term
δ flow rate ($cm^3\ s^{-1}$)
μ molar flow rate ($mol\ s^{-1}$)

Acknowledgment

The authors thank “La junta de Extramadura-Consejeria de Educacion, Ciencia y Tecnologia y el Fondo Social Europeo” for the postdoctoral fellowship given to F.C.-C.

References

[1] C. Vidal-Madjar, F. Cañada-Cañada, I. Gherghi, A. Jaulmes, A. Pantazaki, M. Taverna, J. Chromatogr. A 1042 (2004) 15.
[2] D.S. Hage, S.A. Tweed, J. Chromatogr. B 699 (1997) 499.
[3] C.G. Sanny, J. Chromatogr. B 768 (2002) 75.
[4] C.G. Sanny, J.A. Price, Anal. Biochem. 246 (1997) 194.
[5] J.C.K. Loo, N. Jordan, A. Ho Ngoc, J. Chromatogr. 305 (1984) 194.
[6] K. Murukami, N. Ueno, S. Hirose, J. Chromatogr. 225 (1981) 329.
[7] K. Akasaka, S. Fujii, F. Hayashi, S. Rokushika, H. Hatano, Biochem. Int. 5 (1982) 637.
[8] K. Nakamura, S. Satomura, S. Matsuura, Anal. Chem. 65 (1993) 613.
[9] A. Nimmo, A. Bauermeister, Biochem. J. 169 (1978) 437.
[10] F.J. Stevens, Biophys. J. 55 (1989) 1155.
[11] A. Jaulmes, C. Vidal-Madjar, Anal. Chem. 63 (1991) 1165.